Molecular Crystals and Liquid Crystals
Publication details, including instructions for authors and subscription information:
http://www.tandfonline.com/loi/gmcl16

Polymorphism in Vanadyl Phthalocyanine

C. H. Griffiths [a] , M. S. Walker [a] & P. Goldstein [a]
[a] Xerox Corporation, Webster Research Center, 800 Phillips Road, Webster, New York, 14580
Version of record first published: 28 Mar 2007.

To cite this article: C. H. Griffiths , M. S. Walker & P. Goldstein (1976): Polymorphism in Vanadyl Phthalocyanine, Molecular Crystals and Liquid Crystals, 33:1-2, 149-170

To link to this article: http://dx.doi.org/10.1080/15421407608083878

Mol. Cryst. Liq. Cryst., 1976, Vol. 33, pp. 149–170

Printed in Holland

Polymorphism in Vanadyl Phthalocyanine

C. H. GRIFFITHS, M. S. WALKER and P. GOLDSTEIN

Xerox Corporation, Webster Research Center, 800 Phillips Road, Webster, New York 14580

(*Received August 22, 1975*)

Phase transitions in vanadyl phthalocyanine have been studied using differential scanning calorimetry, x-ray scattering and optical absorption spectroscopy. Three phases, I, II and III, were prepared by nonequilibrium vapour quenching, equilibrium crystal growth and melt quenching, respectively. Phase I is metastable and transforms thermally to Phase II. Both Phase II and Phase III are stable up to the melting point. Phase II has a triclinic crystal structure isostructural with SnPc and is prone to systematic disorder in the ac plane. The disorder enhances the optical absorption at 6500 Å. Attempts to account for the optical absorption spectra using simple dipole–dipole models have been unsuccessful although dimeric structures are suggested for all three phases.

INTRODUCTION

Polymorphism, that is the existence of a chemical compound in more than one crystalline packing arrangement, is a generally common phenomenon. In organic molecular crystals the intermolecular forces are relatively weak and a variety of molecular stacking arrangements of similar energy are often possible. Metal-free phthalocyanine (H_2Pc) illustrated in Figure 1 has been shown to exist in at least three polymorphic modifications[1] (α, β and x) and the central imino hydrogens of H_2Pc can be replaced by a number of metal ions without seriously disrupting the intermolecular interactions. The α, β and x structures isomorphous with those of H_2Pc have been observed in the case of a number of transition metal phthalocyanines.[2,3] Vanadyl phthalocyanine (VOPc) with its more complex oxovanadium cation has received relatively little attention. Assour *et al.*[4] were only able to recognize one single phase using ir spectroscopy and designated this the δ phase. Lucia and Verderame[5] evaporated the Assour material onto heated substrates and again were only able to establish the presence of a single phase by

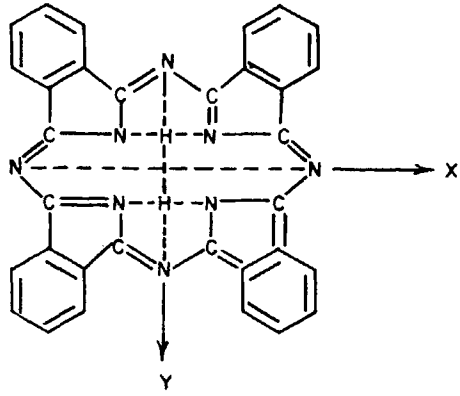

FIGURE 1. Molecular structure of metal-free phthalocyanine.

visible and uv spectroscopy. In this present work we have attempted a more detailed study of polymorphism and structural transitions in VOPc and their influence on optical properties. Thermally induced transitions were monitored by differential scanning calorimetry and the phases characterized using x-ray, ir, visible and uv spectroscopy.

EXPERIMENTAL

VOPc was obtained from Eastman Organic Chemicals. This material was further purified by sublimation in a tube furnace with a flowing argon atmosphere. VOPc was placed in a fused quartz boat at ~430°C and allowed to sublime through a temperature gradient of 20°C/inch onto the walls of the fused quartz furnace tube. The purified material nucleated and grew as rectangular platelets on the tube walls. Single crystals were also grown by slow cooling of saturated solutions of VOPc in quinoline, 1-chloronaphthalene and dimethylformamide. VOPc was prepared for the differential scanning calorimetry (DSC) and the optical absorption study by rapid sublimation at 10^{-5} torr onto room temperature fused quartz substrates. The deposit was scraped off the substrates and weighted samples were sealed in crimped aluminum pans. Thermograms were recorded on a Dupont 900 Differential Thermal Analyzer fitted with a Differential Scanning Calorimeter (DSC) Cell. Calorimetric quantities were calculated from areas under transition peaks measured with a Keuffel and Esser Compensating planimeter. The calorimeter was calibrated using the heat of fusion of lead, indium and tin. Thermally induced structural changes were monitored by

quenching the VOPc samples at points of interest during the thermograms and subjecting these to x-ray diffraction analysis in a Debye–Scherrer camera. Diffraction line intensities and positions were measured with a scanning densitometer. Changes were also followed by uv-visible spectroscopy using a Cary 14 Spectrophotometer with quenched calorimeter samples dispersed in a Nujol mull and coated on a glass slide. The maximum optical density of the mull was adjusted to be approximately 1.0. A separate spectral study of VOPc was conducted using vacuum deposited thin films on quartz for the uv-visible spectra and on KBr for the infra-red spectra which could be monitored directly. This avoided possible problems due to changes induced by the dispersion process and produced better quality spectra. Structural transitions were followed as a function of thermal treatment. Unit cell dimensions of the single crystals were determined using Weissenberg and moving film precession cameras.

RESULTS

a Morphology and Crystal Structure

Crystal growth of VOPc from the vapour phase in an argon atmosphere resulted in rectangular platelets with sizes up to 2 × 1.5 mm and a thickness of about 0.2 mm. In polarized light, however, almost all of these crystals showed twin bands intersecting the large face of the platelet and at $\sim 45°$ to the sides of the platelet. Growth from solution again produced nucleation on the walls of the containing vessel but the crystals were very much smaller in size. X-ray powder scattering patterns from the vapour grown crystals and from each of the three sets of solvent grown crystals were identical. Equilibrium growth conditions produced the same phase regardless of the environment. Samples of the vapour grown single crystals without twin bands were selected and studied in detail. The crystals were found to have a triclinic unit cell containing two molecules with the $P\bar{1}$ space group. The lattice parameters were $a = 12.03, b = 12.58, c = 8.71$ with angles $\alpha = 96.15°$, $\beta = 94.88°$ and $\gamma = 68.16°$. The twin symmetry was determined using twinned crystals and found to be a 180° rotation about the [101] axis.

Non-equilibrium deposition of VOPc from a vapour beam onto fused quartz with the background pressure at 10^{-5} torr produced a film which was largely microcrystalline with some small amorphous character. The diffraction pattern was not similar to that obtained from crystals grown under equilibrium conditions. This phase and its transformation into the equilibrium phase is discussed in the following section.

b Calorimetric Measurements

Both the VOPc phase formed by quenching a molecular vapour beam on a quartz substrate and that produced by equilibrium growth from the vapour were studied by differential scanning calorimetry. The thermally induced structural changes were monitored by x-ray diffraction and uv-visible spectroscopy. In order to minimize the decomposition which occurred at the higher temperatures a heating rate of 40°C/minute was used in the complete scans. Some problems were still encountered with non-reproducible baseline drift in the exothermic direction at temperatures above 400°C. Figure 2 shows a typical thermogram obtained at 40°/minute from the phase quenched from the vapour beam to which corrections have been made for the baseline drift. The trace can be seen to be composed of three exothermic regions; a double peak in the 140–200°C range, a broad peak at 400°C and an exothermic region leading into a sharp endothermic peak with an extrapolated onset at 610°C. This endotherm is followed by a second shallower endotherm and then a change of baseline in the exothermic direction. It was suspected from Figure 2 that the double peak in the 140–200°C range was in fact two overlapping peaks. Careful annealing at temperatures above 100°C showed that the peaks were due to separate processes and that the first process could be taken to completion without significant progress of the second process. Annealing at 135°C for 20 minutes and then quenching back to room temperature before running the thermogram resulted in the

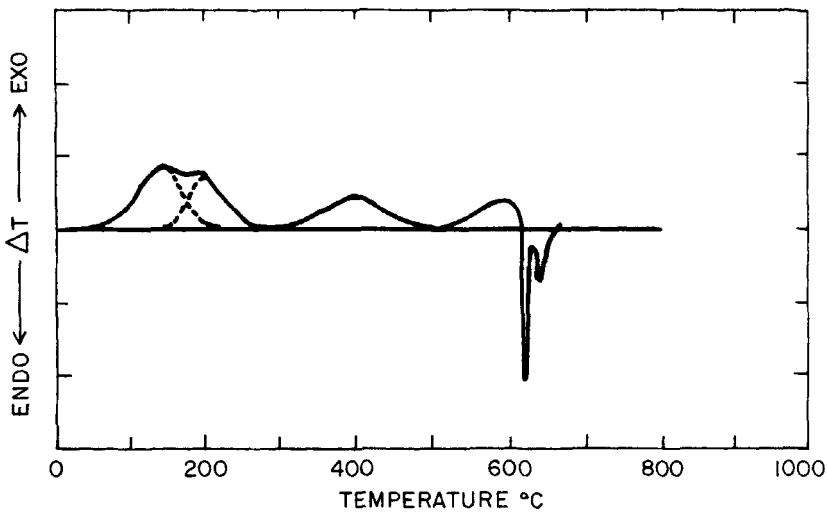

FIGURE 2 Vanadyl phthalocyanine thermogram.

elimination of the first peak at 140°C leaving the peak at 200°C. The two peaks thus resolved are shown by the dashed lines in Figure 2.

The x-ray scattering patterns from the starting material, A, the product of the first exothermic peak, B (135°C for 20 minutes), and the product after the second peak, C, are shown in Figure 3. The starting material (pattern A) had a very small crystallite size with much disorder indicated by the diffuse pattern. Scattering patterns B and C are rather similar indicating that the basic phase change is already complete at the termination of the first exothermic peak. The main differences between B and C are the appearance of new diffraction lines at 10° and 18.7° in the place of diffuse scattering

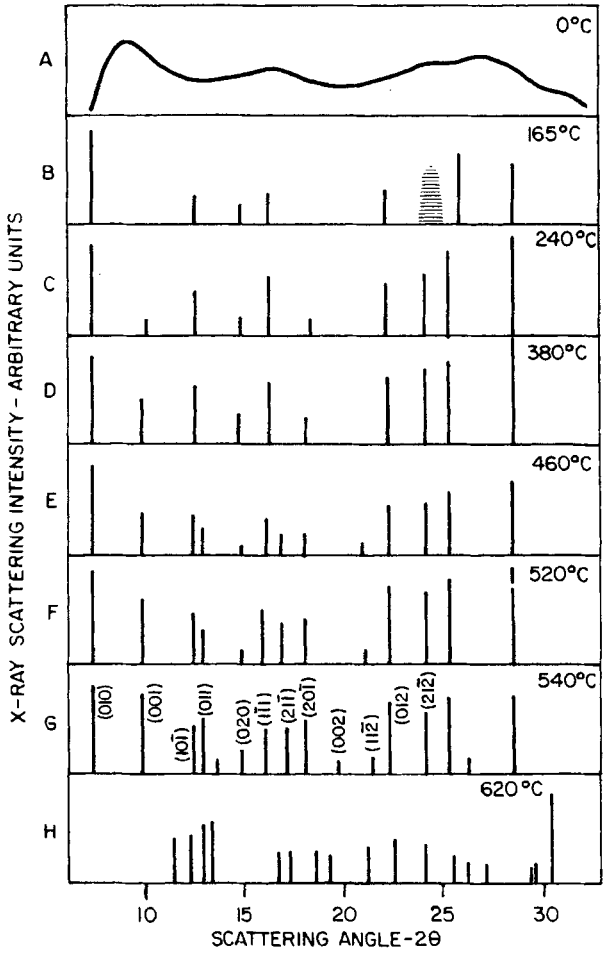

FIGURE 3 X-ray powder patterns from vanadyl phthalocyanine heated at 40°C/minute.

and a shift of the 25.9° line to 25.4° in the pattern C. Some changes in relative line intensities are also visible. It therefore appears that the basic new crystal lattice is generated during the first exothermic peak and that further ordering of the lattice takes place during the second peak. The phase reaction is complete at this heating rate (40°/min) at 275°C.

The third exothermic peak has a maximum at ~400°C, is much more diffuse and encloses a smaller area than the lower temperature peaks. X-ray powder patterns indicate further rearrangements in the molecular structure with changes in line intensity, small shifts in line positions, the appearance of new lines, and decreasing background scattering. These changes, shown in Figures 3D, E and F, continue up to 520°C without any significant increase in crystallite size. At 590°C the x-ray pattern shows increased sharpness and further structure in the diffraction rings indicating that recrystallization has occurred. More low intensity diffraction lines are visible above the decreased background scattering intensity and the diffraction pattern from this material shown in Figure 3G is identical with that obtained from the crystals grown from the vapour phase under equilibrium conditions. Accordingly the diffraction lines of Figure 3G are shown indexed on the basis of the unit cell determined for the equilibrium vapour grown crystals. No indexing has been attempted beyond the $21\bar{2}$ reflection at 3.67 Å due to the large multiplicity of reflections and the lack of relative intensity data. Thermograms measured on these two materials were also very similar. The three exotherms at 140, 200 and 400°C in Figure 2 were no longer visible leaving only the endotherm at 610°C and a second higher temperature endotherm.

Heating of all materials above 590°C led to the first endotherm with the extrapolated onset at 610°C and samples quenced in this range showed obvious physical signs of melting. When the melt was quenched on the recovery arm of the endotherm a new phase with completely different x-ray scattering pattern was obtained. This pattern is shown in Figure 3H. A thermogram run with this phase as the starting material was relatively structureless but had the same melting behavior previously observed for VOPc, i.e., the melting peak at 610°C followed by the second small endotherm illustrated in Figure 2. Visible absorption spectra of this phase dissolved in chlorobenzene were identical with those of the equilibrium vapour grown crystals in the same solvent indicating no significant decomposition of the phthalocyanine. The second endotherm had an extrapolated onset at 630°C and samples quenched in this range had the appearance of a black decomposition residue. X-ray diffraction from this material indicated no crystallinity.

The energies of the exothermic transitions discussed above are proportional to the areas under the transition peaks. In this case the heats of

transition ΔH were obtained from the DSC scans using the formula

$$\Delta H = \frac{E \cdot A \cdot \Delta T_s \cdot T_s}{M \cdot a} \tag{1}$$

where E is the calibration coefficient, A the area under the peak, ΔT_s and T_s the y and x axis sensitivities respectively, M the sample mass and a the heating rate. The calibration coefficient was obtained from samples with known heats of fusion run under identical conditions to the VOPc DSC scans. The calculated ΔH values for the transitions with exothermic peak maxima at 140, 200 and 400°C are shown in Table I. The calculation of ΔH for the transition maxima at 400°C was complicated by the width of the exotherm and the coincident decomposition of VOPc. Only an approximate determination of this value was therefore possible.

TABLE I

Structural transitions of VOPc

	T°C	ΔH cal/gm	
Transition 1 — (a)	140	5.1 ± 0.2	9.1 ± 0.3
(b)	200	4.0 ± 0.2	
Transition 2	400	~3.7	
Melting	610	—	

Absorption spectra were recorded at room temperature for the same quenched VOPc samples used to obtain the x-ray powder patterns. These materials were mulled with Nujol mineral oil as described previously. The resultant spectra are shown in Figure 4. The unheated material has maxima at 6500 Å and 8100 Å and a poorly resolved band at 7200 Å. At 165° the maximum at 6500 Å is enhanced relative to that at 7200 Å and at 240°C the long wavelength maximum is also enhanced relative to 7200 Å and shifted to 8150 Å. Continued heating led to further shifting of the long wavelength maximum. At 460°C the long wavelength absorption maximum had shifted to 8350 Å and some broadening had occurred. This spectrum did not change significantly on further heating until melting occurred. The spectrum of the material quenched from the melt at 620° was however significantly different from those discussed above having a maxima at 7650 and a shoulder near 6700 Å. In all cases the Soret band in these spectra was observed near 3500 Å. These observed spectral changes with thermal treatment were relatively minor other than the case of the phase quenced from the melt. Due to the previously discussed problems with mull spectra no further analysis was attempted.

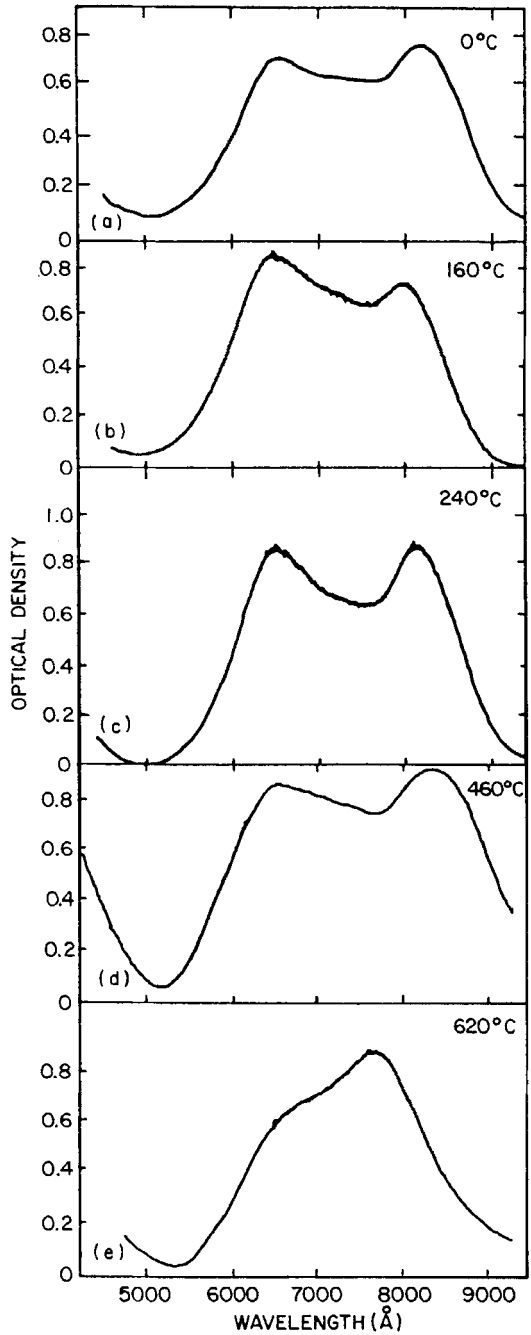

FIGURE 4 Mull spectra from vanadyl phthalocyanine heated at 40°C/minute.

c Thin Film Absorption Spectra

Ultra-violet and visible absorption spectra were recorded for thin films of VOPc prepared by non-equilibrium vapour phase deposition onto quartz slides. Infrared spectra were recorded for similar films deposited onto potassium bromide. These films were prepared together with those used as the starting material for the calorimetric study so that deposition conditions were identical. Unfortunately spectra could not be obtained from the vapour or solution grown crystals due to their small size.

The visible absorption spectrum for a thin film on quartz is shown in Figure 5. The spectrum exhibits a long wavelength band at 7250 Å ($\alpha = 2.1 \times 10^5$ cm^{-1}) with a shoulder at 6700 Å. The Soret band is at 3500 Å ($\alpha = 2.4 \times 10^5$ cm^{-1}) and a shoulder is evident near 2700 Å. It should be noted that this is not identical to the spectrum from the mull of the same material scraped off the substrate shown in Figure 4(*a*). For comparison the absorption spectrum of VOPc dissolved in pyridine (5×10^{-6} M) is also shown in Figure 5. Absorption maxima are located at 6950 Å ($\varepsilon = 9 \times 10^4$ lm^{-1} cm^{-1}) and 6250 Å ($\varepsilon = 1.7 \times 10^4$ lm^{-1} cm^{-1}) with shoulders near 6600 and 5900 Å. The Soret band is near 3500 Å. The infra-red

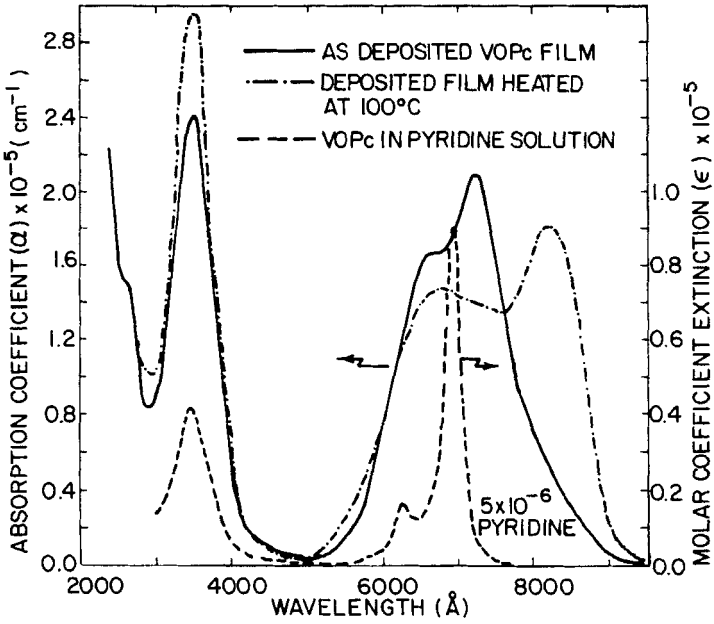

FIGURE 5 Visible absorption spectra for vanadyl phthalocyanine film vacuum deposited on quartz at 25°C, a vacuum deposited film heated at 100°C and a 5×10^{-6} M solution in pyridine.

absorption spectrum (7.5 to 25μ) for the same material as deposited on a KBr substrate is shown in Figure 6. Five vibrational bands are located in the wavelength region 12.0 to 15.0μ. This spectral region was used by Sharp and Lardon[1] to identify the polymorphs of metal-free phthalocyanine. Medium strength bands are also located at 11.08μ, 9.98μ, 8.60μ, 7.92μ and 7.75μ. Strong bands are located in the region 8.8 to 9.4μ. A number of weak bands are also evident.

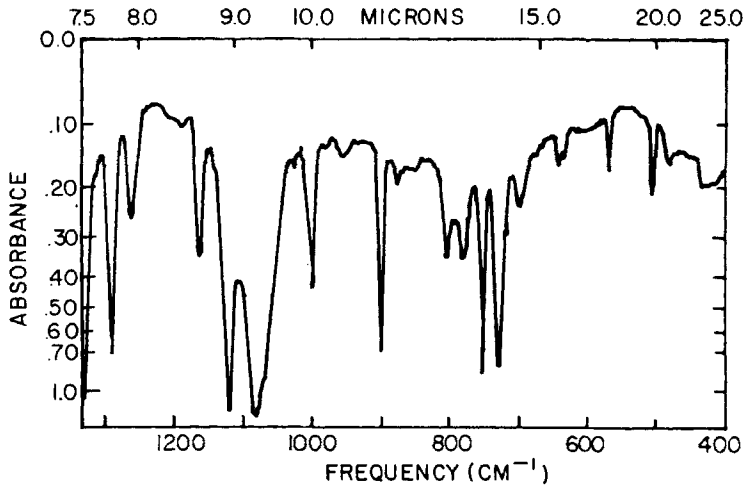

FIGURE 6 Infra-red absorption spectrum of vanadyl phthalocyanine vacuum deposited on KBr at 25°C.

Heating the VOPc film on quartz at 100°C produced a new *near* infrared absorption in the spectrum at 8150 Å ($\alpha = 1.8 \times 10^5$ cm^{-1}) and a change in the relative intensities of the 7250 Å and 6700 Å peaks. The spectra of the film after 1 and 4 hours at 100° are shown in Figure 7. The spectrum of the new phase is shown in greater detail in Figure 5. The infrared spectrum exhibited some changes after heating at 100°C. These were confined to an increase in the intensity of the band at 11.4μ, other minor intensity changes and a small shift to shorter wavelength ($\sim$.03μ) of several bands.

No obvious changes were noted in the uv-visible spectrum of these films when further heated at 250°C, however some changes were noted in the ir spectrum (Figure 8). The bands at 7.9μ, 12.5μ and 14.3μ are significantly reduced in intensity while the band at 12.8μ is resolved into a doublet.

Heating of the films above 300°C resulted in band broadening in the uv-visible spectrum with a shift of the long wavelength maxima to 8300 Å and a decrease in the relative intensities of the 7250 Å and 6700 Å bands, Figure 9. A visual observation of the VOPc film indicated significant crystal

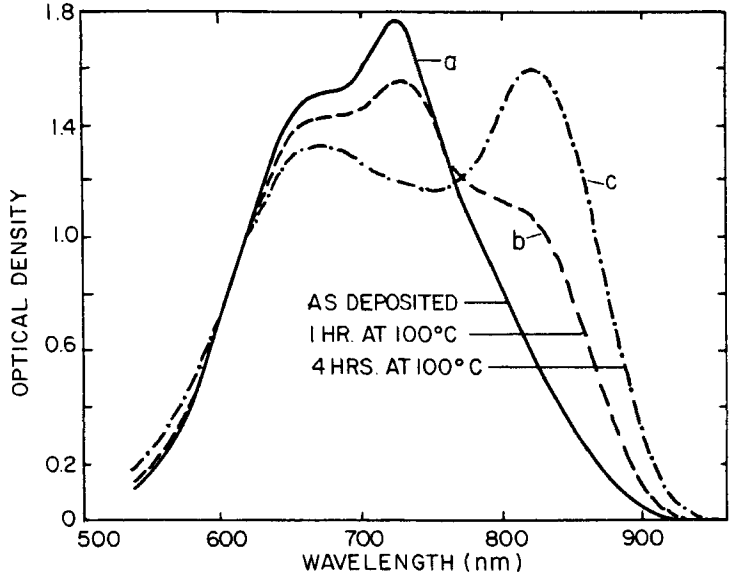

FIGURE 7 Visible absorption spectra from vanadyl phthalocyanine film on quartz (a) before heating, (b) after heating at 100°C for 1 hour, (c) after heating at 100°C for 4 hours.

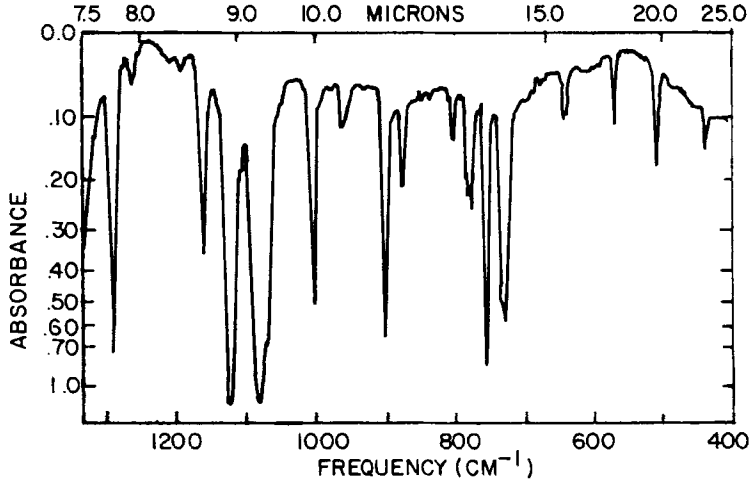

FIGURE 8 Infra-red absorption spectrum of vanadyl phthalocyanine on KBr heated at 250°C for 2 hours.

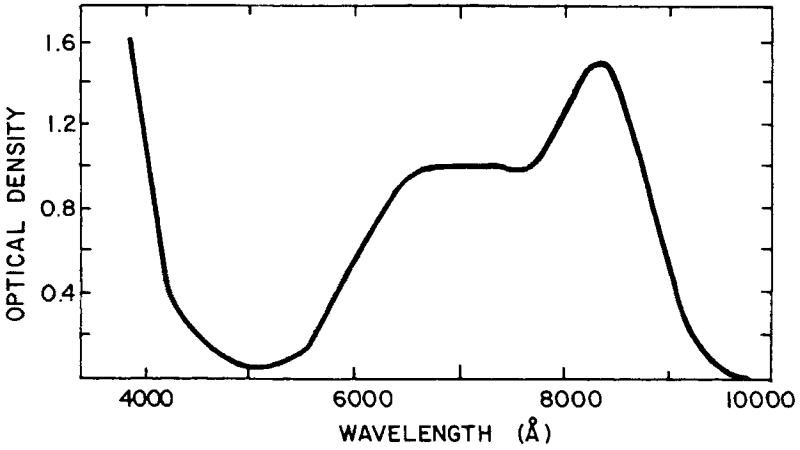

FIGURE 9 Visible absorption spectrum of vanadyl phthalocyanine film on quartz heated at 325°C for 2 hours.

growth which possibly accounts for some of the band broadening, i.e., due to light scattering. The infra-red spectrum of the material on KBr, indicated no significant change from that shown in Figure 8, except again for some minor intensity changes. Transition energies in the long wavelength spectra of VOPc are summarized in Table II.

DISCUSSION

The differential scanning calorimetry technique indicates that VOPc prepared by non-equilibrium vapour quenching undergoes three distinct exothermic transitions prior to melting. These are shown as transitions 1(*a*), 1(*b*) and 2 in Table I. X-ray powder diffraction analysis however does not confirm that these exothermic transitions are all the result of abrupt structural transformations. Transition 1(*a*) does result in a radical change in the x-ray scattering but further heating below the melting point results in an evolution of the pattern rather than any abrupt change. This evolution results in small shifts in the position of lines, changes in relative intensities, the appearance of new lines and a sharpening up of lines together with a gradual reduction of background scattering. These evolutionary changes illustrated diagrammatically in Figure 3 are more marked at the temperature ranges of the exotherms shown in Figure 2. The final product of these evolutionary processes is a diffraction pattern identical to that obtained from equilibrium solution grown crystals.

The non-equilibrium vapour quenched starting material was determined by transmission electron microscopy to be largely microcrystalline and has a

diffraction pattern which is distinctly different in the positions of its maxima from the products of the thermally induced transitions. This material, although not well characterized by its x-ray scattering pattern, will be referred to as Phase I. The uv-visible absorption spectrum of a thin film of Phase I on quartz is shown in Figure 5.

Heating of Phase I resulted in an exothermic transition (1(*a*) of Table I) and the establishment of a new scattering pattern which appears to be the result of a new state of crystallographic order. This material will be referred to as Phase II. The background scattering in the x-ray pattern from this material was high and the lines were rather diffuse. As previously discussed further heating led to a reduction in background scattering, the sharpening up of existing diffraction peaks and the appearance of new ones. This evolution which finally resulted in a scattering pattern identical to that from equilibrium grown crystals appeared to involve two distinct processes, transition 1(*b*) and transition 2. The sharp fully developed Phase II pattern

TABLE II

Optical transition energies

Phase	Energy (cm^{-1})				
Molecular (solution)	—	—	14,390(0′–0″ transition)		
Vac. evap. (I)	—	(15,040)	—	13,790	—
Heated, 100°C. (II)	(16,236)	14,815	—	(13,700)	11,980
Heated 325 C. (III)	—	(14,925)	—	13,070	—

Brackets denote estimated peak positions, error ± 200 cm^{-1}.

shown in Figure 3G was indexed on the basis of the single crystal structure determined from equilibrium vapour growth crystals and an attempt was made to correlate the exothermic transitions and the corresponding appearance of new diffraction peaks and changes in relative peak intensities with the elimination of disorder in specific planes. Without a complete crystal structure determination no quantitative analysis involving diffraction line intensities was possible. Certain changes involving relative intensities are however obvious. The second exothermic peak (transition 1(*b*)) is characterized by the appearance of the previously absent (001) and (20$\bar{1}$) reflections and the sharpening up of the (21$\bar{2}$). Further heating results in increasing intensity in the (001) reflection and finally the appearance of the second order (002) reflection at 590°C. At 460°C the (011), (21$\bar{1}$) and (11$\bar{2}$) reflections also appear and increase in intensity up to 590°C.

Although a complete structure determination for VOPc (Phase II) is not available, this material has the same space group as that published for Sn^{2+} phthalocyanine[6] and the lattice parameters are almost identical. The relevant

TABLE III

A comparison of lattice parameters for vanadyl and tin phthalocyanines

	a	b	c	α	β	γ	Number of molecules per unit cell	Space group
VOPc	12.032	12.579	8.712	96.15	94.88	68.16	2	$P\bar{1}$
SnPc[6]	12.060	12.618	8.675	95.89	95.08	68.17	2	$P\bar{1}$

parameters for the two phthalocyanines are given in Table III. Based on this great similarity in each known aspect of the structures it is reasonable to assume that the large phthalocyanine molecules have the same fractional coordinates in the two cells and that the small differences are due to the size of the cation. In tin phthalocyanine the tin atom is 1.1 Å above the centroid of the four central N atoms of the phthalocyanine molecule.[6] If in VOPc the V—N and V—O distances are assumed to correspond to those in a similar vanadyl porphyrin, vanadyl deoxophyllaerythaoetioporphyrin-1,2-dichloroethane solvate,[7] then the vanadium atom will be 0.70 Å above the centre of the plane bordered by the four nitrogen atoms and the oxygen atom 1.62 Å above this. Using the fractional coordinates for the phthalocyanine molecule in the tin phthalocyanine structure deduced by Mason,[8] the coordinates of the vanadyl phthalocyanine molecule within the unit cell were calculated. A projection of the calculated structure down the *b* axis onto the *ac* plane is shown in Figure 10. Due to the large size of the phthalocyanine molecule only the four central nitrogen atoms are shown to indicate the plane of the molecule. The unit cell contains two molecules, marked 1 and 2, and the centroids of these molecules are respectively 0.51 Å in front and behind the illustrated *ac* plane. All the phthalocyanine molecules are parallel and the distances between their centroids are given in Figure 10. The angle between the line joining the centroids of the closest pair of phthalocyanine molecules (the pair at 5.1 Å) and the plane of either phthalocyanine molecule is 65.5°.

If the changes in diffraction line intensities illustrated in Figure 3 are considered in terms of the structure for VOPc proposed above they can be understood on the basis of structural ordering. The transition evidenced by the second exothermic DSC peak results in x-ray pattern C which contains the previously absent (001) and ($20\bar{1}$) reflections while the (010) reflection intensity is unchanged. This indicates a reduction in disorder within the *ac* planes while the degree of order between these planes is maintained. Disorder within the *ac* plane will be the result of a lack of regularity in the arrangement of the closest packed VOPc molecules at 5.1 and 8.8 Å. This state of disorder is basically maintained up to the transition (transition 2) evidenced by the exothermic peak at ~400°C. At this point further ordering takes place which results in the appearance of missing reflections from planes intercepting the

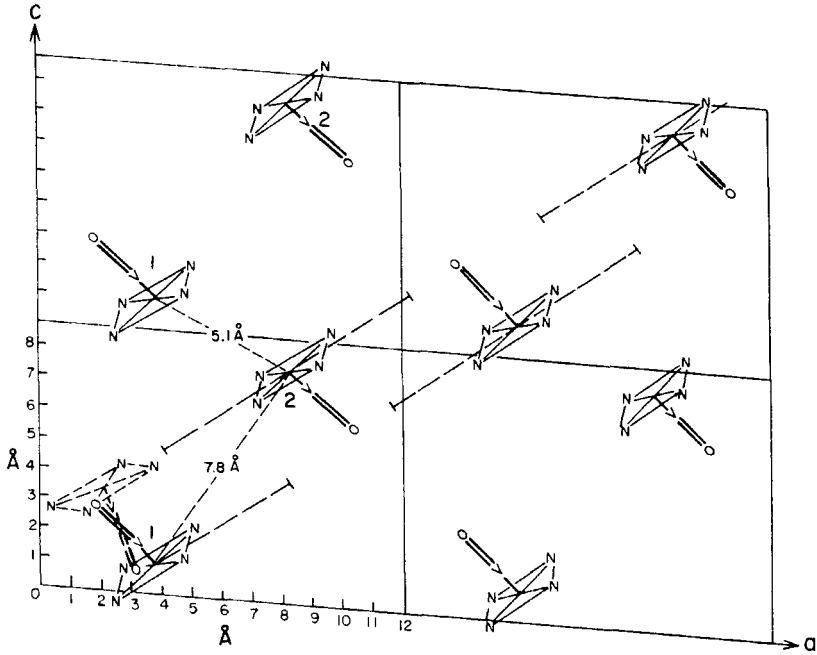

FIGURE 10 Structural model for Phase II VOPc showing also the ac plane disorder produced by the 180° rotation about the [101] twin axis (dotted lines). Dashed lines show the actual diameter of the phthalocyanine molecule.

b-axis, apparently a secondary result of the *ac* plane ordering. Further heating increases the relative intensity of these reflections and also the (001) and (20$\bar{1}$) which initially appeared at 240°C. These ordering processes in the *ac* plane culminate in the appearance of the second order 002 reflection at 590°C.

From the above it is evident that the VOPc Phase II crystal lattice is prone to defective packing in the *ac* plane. As pointed out previously macro-twinning was observed in almost all vapour grown VOPc single crystals. The two members of the twin pair being related by a 180° rotation about the [101] axis. This twinning if present on a microscale, would produce stacking disorder in the *ac* plane which could account for the missing reflections in the x-ray scattering patterns illustrated in Figure 3. It seems reasonable to conclude therefore that the energy differences between the twinned and perfect molecular packing configurations are relatively small. This is apparent from the difficulty in obtaining untwinned single crystals. The result of this is that when Phase II is produced from Phase I at temperatures of 250°C and below, considerable disorder of this type and possibly other types will be present. The stacking disorder described above is indicated by the VOPc molecule drawn with dashed lines in Figure 10.

The uv-visible spectra of the Phase II VOPc as a function of thermal treatment shown in Figure 4(*b*), (*c*) and (*d*) give definite indications of some reorganization of the crystal lattice but no direct knowledge as to its nature. These spectra are generally similar to those of the thermally treated thin films except for some variation in band intensities. Consideration of Figure 4(*a*), (*b*) and (*c*) and Figure 9 shows a concomitant decrease in the relative intensity of the 6500 to the 8150 Å transition as the defect concentration decreases due to thermal annealing. This observation suggests that the absorption is perturbed by the molecular interactions in the defective lattice structure. The fact that the intensity of the 6500 Å transition relative to that of the 8150 Å transition in the bulk DSC generated materials is always higher than that in the thermally converted thin film supports this picture. The DSC generated materials all suffer considerable mechanical damage during the mulling process which probably results in the generation of numerous lattice defects. The spectrum of the VOPc film heated above 300°C (Figure 9) exhibits the lowest relative intensity of the 6500 Å transition and is similar to that reported by Lucia and Verderame[5] for VOPc vacuum deposited onto heated ($\sim$150°C) substrates. Deposition onto the heated substrate may allow sufficient surface diffusion for the formation of relatively defect-free Phase II VOPc.

The spectrum of the unheated starting material in Figure 4(*a*) is not markedly different from the Phase II material. Apparently the action of grinding the Phase I VOPc to form the Nujol mull causes the Phase I $\rightarrow$ Phase II transformation. The true spectrum of Phase I VOPc obtained from an as-deposited film is shown in Figure 7.

The third crystallographically distinct phase of VOPc, referred to from this point as Phase III was obtained only by quenching from the melt but was apparently stable when heated to the melting point. The relative stabilities and melting points of Phases II and III could not be determined with any certainty, but they apparently have similar free energies close to the melting point.

As discussed above the form of VOPc prepared by non-equilibrium vapour quenching is assigned as Phase I. The long wavelength visible absorption band of this phase consists of two components (6700 and 7800 Å) separated by some $\sim 1100\ cm^{-1}$. This separation is comparable to that observed in the long wavelength absorption band of the α polymorphs of metal-free and transition metal substituted phthalocyanines. For the latter phthalocyanines these transitions have been attributed to exciton splitting of the degenerate O′—O″ molecular transition.[9] It is unlikely that the 6700 Å band is a vibrational component as examination of the molecular spectrum of VOPc indicates a vibrational splitting of $\sim 750\ cm^{-1}$ (see Table II).

Lucia *et al.*[5] have reported a side band in the spectrum of matrix isolated copper phthalocyanine which they attribute to a dimeric specie. More recently Monahan *et al.*[10] have studied the dimerization of phthalocyanine dyes, including vanadyl tetraalkylphthalocyanine, in solution. These authors pointed out the similarity between the absorption spectrum of the dimer in solution and that of the solid state polymorph prepared by vacuum deposition[10] and suggested that the crystal structure of the dye was also dimeric. Extension of this analogy to the VOPc Phase I spectrum suggests that the crystal packing in this polymorph may also be dimeric in nature. Single crystal x-ray spectra are unfortunately not available for the Phase I vanadyl phthalocyanine to establish the crystal structure unambiguously. The splitting, which would be a measure of the interaction energy in the dimer,[12] is less for VOPc ($\sim 1100\ cm^{-1}$) than for the α polymorphs of metal-free ($1761\ cm^{-1}$), cobalt ($1634\ cm^{-1}$), nickel ($1554\ cm^{-1}$), copper ($1963\ cm^{-1}$) and zinc ($1346\ cm^{-1}$) phthalocyanines. This difference could be accounted for by a somewhat larger spacing of the molecules in a VOPc dimer due to the increased size of the vanadyl cation. This observation is contrary to that for the phthalocyanine dyes reported by Monahan *et al.*[10] where the vanadyl spectrum exhibits a greater splitting than those of the zinc and copper derivatives.

Dimerization of vanadyl porphyrins has also been reported. Boyd *et al.*[13] have estimated the metal ion–metal ion spacing in the vanadyl porphyrin dimer to be about 3.7 Å, whilst Dickson and Petrakis[14] have suggested a porphyrin–vanadium co-ordinated dimer structure.

The visible absorption spectrum of the Phase II material is similar to that of the x-polymorphs of metal-free and copper phthalocyanine. Sharp and Lardon[1] have interpreted the spectrum of the x forms of phthalocyanine as being due to dimerization. They were able to resolve four component absorption bands in the long wavelength spectrum of x-metal-free phthalocyanine which they attributed to exciton splitting of the M and L axis polarized low energy transitions. Their calculation using the exciton dipole–dipole approximation gave an intermolecular separation of 4 Å. This calculated value may be compared to the measured (x-ray structure analysis) values of 4.7 Å for the intermolecular separation in β-metal-free phthalocyanine.[15]

If we accept that both Phase I and II are dimeric in structure then it is necessary to explain the observed differences in the respective absorption spectra.

The lowest unoccupied molecular orbital in metal phthalocyanines of D_{4h} symmetry is degenerate.[16] This is apparently the case for VOPc having a C_{4v} symmetry as indicated by the single long wavelength transition

observed in the molecular spectrum (Figure 5). This degeneracy is removed in metal-free phthalocyanine because of the lower D_{2h} symmetry of this molecule and both transitions are observed in the molecular spectrum.

If we assume that the Phase I VOPc is dimeric then the transitions at 13790 cm^{-1} and $\sim$15040 cm^{-1} correspond to the $\pm$ components resulting from splitting of the molecular O′—O″ transition located at 14390 cm^{-1} (pyridine solution). If this latter transition is degenerate then the degeneracy is apparently retained under dipole coupling, or alternatively the components are not resolved in the measured spectrum. The simplest structure which might account for the observed spectrum is that of a *parallel plane* dimer.

Using the dipole–dipole[17] approximation the splitting (ΔE) for a *parallel plane* dimer is related to the transition dipole strength (D), the intermolecular spacing (R) and the angle between the transition dipoles (α_{12}) by

$$\Delta E = \frac{2D}{R^3} \cos \alpha_{12} \text{ ergs.} \tag{2}$$

The dipole strength can be calculated from

$$D = \frac{3he^2}{8\pi^2 m_e c g_n \nu_{mn}} \rho_{mn} \text{ erg cm}^3 \tag{3}$$

where ρ_{mn} is the oscillator strength calculated by integration of the corresponding molecular absorption band

$$\rho_{mn} = 4.32 \times 10^{-9} \int_{\nu_1}^{\nu_2} \varepsilon \, dV \text{ erg cm} \tag{4}$$

ν_{mn} is the transition frequency and g_n the degeneracy of the excited state. Any interpretation of the crystal structure of VOPc using this model can only be regarded as qualitative as the model applies to the case where the transition dipole length is small compared with the dimer intermolecular spacing. This is not the case for VOPc where the dipole length is comparable to or greater than the intermolecular spacing (Figure 10).

Integration of the 14390 cm^{-1} molecular transition gives a value of 3.5×10^{-1} erg cm for the oscillator strength. Substitution of this value into Eq. (3) gives a value of 2.6×10^{-35} erg cm^3 for the dipole strength of the transition, assuming degenerate transitions of equal intensity, i.e., $g_n = 2$.

Using the calculated dipole strength, a value of 3.7 Å for the intermolecular spacing (cf Ref. 13) and the measured splitting of $\sim$1200 cm^{-1}, a value of 77° for the angle between the transition dipoles is calculated using Eq. (2). This angle is the same for both the M and L transitions in the dimer as the transitions are orthogonal in the single molecule. This proposed dimer structure for VOPc Phase I is shown schematically in Figure 11(a). In this

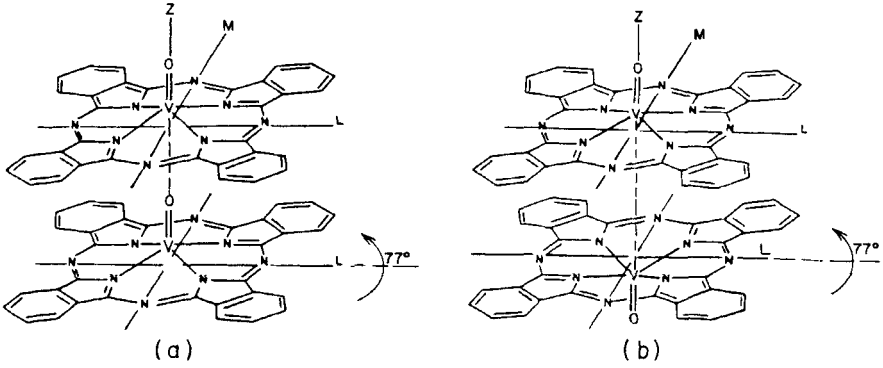

FIGURE 11 Proposed Phase I VOPc dimeric structure, parallel plane rotated configuration.

structure the V=O bonds are aligned in the same direction. An alternate configuration is where the V=O bonds are aligned in opposite directions, Figure 11(b).

Four transitions are evident in the absorption spectrum of Phase II material (Table II) suggesting a further lowering of the molecular symmetry in the dimer. An examination of the postulated crystal structure of Phase II (Figure 10) indicates no dimeric specie with an intermolecular spacing of the order of 3 to 4 Å. A parallel plane inclined dimeric structure (closest pair) with an intermolecular separation of 5.2 Å and a tilt angle of 65.5° is, however, evident.

The splitting (ΔE), again using the dipole-dipole approximation,[16] for this dimeric structure as shown in Figure 12 is given by

$$\Delta E = \frac{2D}{R^3}(1 - 3\cos^2\theta) \tag{5}$$

where θ is the tilt angle.

Substitution of the corresponding values for D, R and θ into Eq. (5) leads to values for ΔE of 900 cm^{-1} and 1860 cm^{-1} for the splitting of the M and L transition respectively, θ being respectively 65.5° and 90°. These calculated splittings are too small to account for the actual spectrum of II. For a true parallel plane tilted dimer with $\theta > 54°$ the high energy component would have the greatest intensity. The closest pair in Figure 10 are in fact displaced some 1 Å with respect to each other which might, from symmetry considerations, lead to both the high and low energy transitions appearing in the spectrum. The dimer intermolecular spacing would, however, have to be of the order of 3.5 Å for this model to account for the observed splittings in the spectrum of Phase II. A consideration of the assumptions which are necessary for the dipole-dipole approximation to account for the spectrum of Phase II

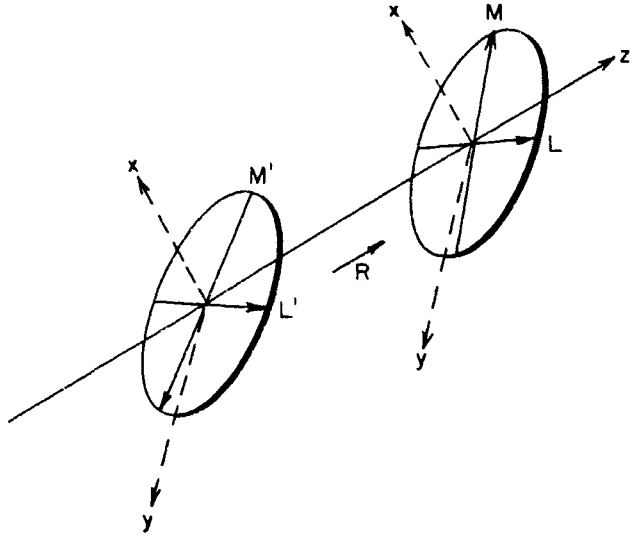

FIGURE 12 Possible Phase II VOPc dimeric structure, tilted parallel plane configuration.

points out the poor approximations of the model in this case. A more refined calculation of the transition energies in the vanadyl phthalocyanine crystal spectra should take into account both dipole–dipole and charge transfer interactions. It is of interest to note that the Phase II VOPc proposed structure is composed of sheets of parallel and overlapping VOPc molecules with a separation of ~3 Å and a spacing of 7.6 Å between centroids.

Finally the spectrum of the Phase III bulk material is similar, though red shifted some 700 cm^{-1}, to that of the Phase I film (Table II). The splitting for this phase is, however, approximately 1900 cm^{-1}. This material did not convert to Phase II on heating, suggesting a more stable form of VOPc than Phase I. Again it is suggested that the crystal structure is dimeric in nature with possibly a somewhat smaller intermolecular distance than Phase I.

The infra-red spectra provide little structural information, unlike the infra-red spectra of the polymorphs of metal-free phthalocyanine which show significant band and intensity changes near 12–15μ. The band at 9.98μ observed in the infra-red spectrum of vanadyl compounds has been assigned to the V—O stretching frequency. Dickson and Petrakis[14] reported shifts in this band in the spectrum of vanadyl porphyrin which they attributed to V—O—V co-ordination. Assignment of the 9.98μ transition in the spectrum of the vanadyl phthalocyanine is, however, made ambiguous by the observation of a transition at similar energies in the spectrum of metal-free and transition metal phthalocyanines.

CONCLUSIONS

Calorimetric, x-ray and spectral data all indicate that vanadyl phthalocyanine (VOPc) can exist in three distinct polymorphic forms. These polymorphs have distinctive x-ray scattering patterns and optical absorption spectra. Phase I results from non-equilibrium quenching of a VOPc vapour beam; Phase II is produced by crystal growth from the vapour and from solution under equilibrium conditions and by heating Phase I at temperatures of $\sim 200°C$ and above; Phase III is formed by quenching from the melt at $\sim 610°C$. Both Phase II and Phase III were stable up to the melting point. The crystal structures of Phases I and III were not determined due to a lack of suitable single crystals. Phase II was found to be triclinic with $P\bar{1}$ symmetry but often existed with considerable systematic disorder. This disorder was severe in the *ac* plane and could be interpreted as due to a micro-scale twinning mechanism involving a 180° rotation about the [101] axis. The positions of the VOPc molecules within the unit cell were not determined experimentally but were calculated on the basis of the positions of the phthalocyanine molecules in the unit cell of the isostructural SnPc.

The visible and infra-red spectra support the interpretation based on the x-ray line analysis of the three phases of vanadyl phthalocyanine. The variations in band intensity in the visible spectrum observed on heating through 300°C could be accounted for by changes in the defect structure of the material. Nujol mull spectra are apparently not representative of the true material due probably to a reintroduction of lattice defects during sample preparation which modulate the absorption spectra. The simple dipole–dipole models are insufficient to clearly account for the Phase II spectrum though dimeric structures are suggested for this phthalocyanine similar to that proposed earlier by Sharp *et al.* for x metal-free phthalocyanine.

Acknowledgements

The writers wish to acknowledge many helpful discussions with A. R. Monahan and R. Gruber and also express their appreciation to R. Gruber for supplying samples of the different polymorphs of vanadyl phthalocyanine. They also wish to thank R. Bigelow and P. Vernon who carried out much of the experimental work involved in this study.

References

1. J. H. Sharp and M. Lardon, *J. Phys. Chem.*, **72**, 3230 (1968).
2. R. P. Linstead and J. Monteath Robertson, *J. Chem. Soc.*, 1736 (1936).
3. J. H. Sharp and M. Abkowitz, *J. Phys. Chem.*, **77**, 477 (1973).
4. J. M. Assour, J. Goldmacher and S. E. Harrison, *J. Chem. Phys.*, **43**, 159 (1965).
5. E. A. Lucia and F. D. Verderame, *J. Chem. Phys.*, **48**, 2674 (1968).

6. M. K. Friedel, B. F. Hoskins, R. L. Martin, and S. A. Mason, *Chem. Communications*, 400 (1970).
7. R. C. Pettersen, *Acta Cryst.*, **B25**, 2527 (1969).
8. S. A. Mason, Ph.D. Thesis, Melbourne University (1971).
9. L. E. Lyons, J. R. Walsh and J. W. White, *J. Chem. Soc.*, **167** (1960).
10. A. R. Monahan, J. A. Brado and A. F. DeLuca, *J. Phys. Chem.*, **76**, 1944 (1972).
11. M. Abkowitz and A. R. Monahan, *J. Chem. Phys.*, **58**, 2281 (1973).
12. A. S. Davydov, *Theory of Molecular Exitons*, Nauka Press, Moscow 1968, page 56.
13. D. D. W. Boyd, S. D. Smith, J. H. Price, and J. R. Pilbrow, *J. Chem. Phys.*, **56**, 1253 (1972).
14. F. E. Dickson and L. Petrakis, *J. Chem. Phys.*, **74**, 2850 (1970).
15. J. M. Robertson, *J. Chem. Soc.* 615 (1935), 1195 (1936), 219 (1937).
16. I. Chen, *J. Mol. Spectroscopy*, **23**, 131 (1967).
17. M. Kasha, H. R. Rawls and M. A. El-Bayoumi, *Pure and Appl. Chem.*, **11**, 371 (1965).